Carotid Ultrasound Segmentation Using DP Active Contours

Ali K. Hamou[1], Said Osman[2], and Mahmoud R. El-Sakka[1]

[1] Computer Science Department
University of Western Ontario, London, ON, Canada
{ahamou, elsakka}@csd.uwo.ca
[2] St. Josephs Health Sciences Centre, London, ON, Canada
said.osman@sjhc.london.on.ca

Abstract. Ultrasound provides a non-invasive means for visualizing various tissues within the human body. However, these visualizations tend to be filled with speckle noise and other artifacts, due to the sporadic nature of high frequency sound waves. Many techniques for segmenting ultrasound images have been introduced in order to deal with these problems. One such technique is the active contouring.

In this paper, two proposed alterations to the dynamic programming parametric active contour model (or snake) are introduced. The first alteration allows the snake to converge to the one-response result of a modified Canny edge detector. The second provides a function that allows a user to preset *a-priori* knowledge about a given object being detected, by means of curve fitting and energy modification. The results yield accurate segmentations of cross-sectional transverse carotid artery ultrasound images that are validated by an independent clinical radiologist. Utilizing the proposed alterations leads to a reduction of clinician interaction time while maintaining an acceptable level of accuracy for varying measures such as percent stenosis.

Keywords: Ultrasound Imaging, Carotid Stenosis, Image Segmentation, Active Contour Models.

1 Introduction

Carotid ultrasound (US) is considered an inexpensive non-invasive clinical procedure for evaluating many carotid artery diseases [10]. It provides flexibility for offline review of patient records efficiently, i.e., the US images can be acquired by a clinician and stored for later testing and analysis, with minimal user input. A brightness-mode (or B-mode) US image is one of the two major types of US used on the carotid. This study will primarily focus on B-mode images since it provides an adequate means for an efficient clinical measurement of patients that are susceptible to plaque accumulation (whether from diet, genetics, obesity, etc). A B-mode US image is made up of a two-dimensional ultrasound display composed of bright pixels representing the ultrasound echoes and reverberations [16]. The echo amplitude determines the brightness of each pixel.

M. Kamel and A. Campilho (Eds.): ICIAR 2007, LNCS 4633, pp. 961–971, 2007.

A high degree of carotid artery stenosis, which can be used as a pre-clinical disease marker, is an early indicator of a possible stroke. Stenosis is the abnormal narrowing of a blood vessel. It is generally caused by plaque build up [10]. Atheromatous plaque is an accumulation of fatty deposits that form inflamed patches within the inner lining of the arteries. In ultrasound images, hard (calcified) and soft plaque are represented as a range of high and low contrast pixels. However, these plaque areas have virtually the same levels of contrast to the surrounding soft tissue due to the lack of texture resolution and the high levels of noise inherent to US images. This poses many difficult problems for plaque and lumen detection algorithms since experienced clinicians subjectively dictate the amount of plaque build up based on knowledge of image structures and prior training.

Boundary detection is one of the most important elements of computer vision. Many techniques have been introduced to accomplish this task. One such example is an active contour model. Kass *el al.* [11] first proposed the original active contour model, also commonly known as a snake or a deformable model. In their formulation, image segmentation was posed as an energy minimization problem.

Active contours treat the surface of an object as an elastic sheet that stretches and deforms when external and internal forces are applied to it. These models are physically-based, since their behaviour is designed to mimic the physical laws that govern real-world objects [8]. This model helps solve the problems of edge based segmentation techniques, such as bleeding of the contour and unstable borders as exhibited in [1].

Active contour models have two inherent problems:

- *the proximity limitations of attaining a true boundary, especially when coupled with poor initialization plots*
- *the inability of traversing boundary concavities due to strong surface tension in the curve.*

The former is rarely an issue in the medical arena since clinicians are generally accepted as experts. Conversely, several studies have been conducted to overcome the latter, while also improving the accuracy and the speed of the original design. Of these are Dynamic Programming (DP) [5], level sets [18] and Gradient Vector Flow (GVF) models [19] just to name a few.

The DP parametric active contour provides an efficient algorithm to quickly attain a desired curve. In this study, we have chosen this model for this attractive feature. Within this model, we propose a new external energy to be made up of two distinct elements. The first is to be composed of an edge map resulting from a modified Canny edge detector. Canny edge detection will maintain the one-edge response and the local connectedness property of an image, whereas the active contour will ensure that our entire energy is minimized over the detected border [5]. The second will be the curve-fitted data built upon the user's initial plots and incorporated into the energy. This will amplify the amount of knowledge received from the clinician in acquiring a desired boundary.

The proposed segmentation algorithm is used to extract a cross-sectional area of the carotid artery at two specified positions (see Section 2.3), which is then used to calculate a percent stenosis that is less prone to user bias between clinicians. It is important to note that measuring the percent stenosis is usually done by manually estimating the diameter of the carotid via catheter angiography. This introduces large user bias into the calculations, while being quite costly from a clinician's time standpoint.

Abolmaesumi *et al.* [4] designed an efficient Kalman-star algorithm to estimate the location of the arterial wall. However, their algorithm still crosses the external boundaries of the wall due to the use of first degree gradient estimation.

Mao *et al.* [13] used a contour probability distribution (CPD) function in order to evaluate the accuracy of their segmentation algorithm. Their algorithm employed entropy mapping and morphological operations based on gray-level values within an image. These mappings create an accurate identification of the arterial wall. However they are strenuous on computer systems resulting in long execution times.

A class of schemes [1][2][3][9] for carotid artery contour extraction that are based on the use of local edge detection techniques are proposed. However, these schemes are used globally throughout an image, and hence lack localization. All of these techniques are susceptible to leaking (or contour bleeding), especially if the image quality is not suitable. Hence other means are needed to properly segment the carotid and calculate its percent stenosis.

The rest of this paper is organized as follows. In Section 2, the proposed scheme is presented. The results of the scheme are shown in Section 3, and Section 4 contains conclusions.

2 System and Methods

2.1 External Energy Formulation

A snake is an energy minimization problem. Its energy is represented by two forces (internal energy, $\boldsymbol{E}_{in}$, and external energy, $\boldsymbol{E}_{ex}$) which work against each other. The total energy should converge to a local minimum – in the perfect case – at the desired boundary. The snake is defined as *X(s)*, where *s* belongs to the interval [0,1]. Hence, the total energy to be minimized to give the best fit between a snake and a desired object shape is:

$$\text{Total Energy} = \int_{s=0}^{s=1} \{E_{in}(X(s)) + E_{ex}(X(s))\} ds \tag{1}$$

The internal energy would force the curve to be smooth (by incorporating both elasticity and stiffness); whereas the external energy would force the curve towards image structures (image edges). The internal energy of the active contour formulation is further defined as:

$$E_{in}(X(s)) = \alpha \times \left(\frac{dX(s)}{ds} \right)^2 + \beta \times \left(\frac{d^2 X(s)}{ds^2} \right)^2 \tag{2}$$

where α and β are the weights of elasticity and stiffness, respectively. The first order term makes the snake's surface act like a membrane. The weight α controls the tension along the spine (stretching a balloon or elastic band). The second order term makes the snake act like a thin plate. The weight β controls the rigidity of the spine (bending a thin plate or wire) [8]. We define our external energy as:

$$E_{ex} = \gamma \times Canny(f(x,y), \sigma, l, u) + \tau \times Shape(X(s)) \quad (3)$$

where γ and τ are the weights for the two proposed external energy elements, Canny and prior shape knowledge, respectively, and $f(x,y)$, σ, l, and u, represent the original image and the parameters for the Canny operator, being the degree of Gaussian blur, a lower threshold and an upper threshold. The weights γ and τ are important factors in governing whether the clinician's knowledge or the modified Canny edge map takes precedence in the converging snake model.

In general, active contour internal and external energies need to be balanced properly in order to converge to the desired edge in question. In order to properly tune the given curve with the proper weights, values were adjusted until the snake converged to the edges chosen by the radiologist. Samples were taken on both normal and diseased images in order to properly validate the curve with the chosen weights. Initially, equal weights were assigned to each energy. Gradually weights were shifted until acceptable edge convergence was achieved. The weights α, β, γ and τ were set to 0.09, 0.01, 0.5, and 0.4, respectively. This is justified for the US images, since the modified Canny edge detector and the a-priori knowledge resides in the external energy formulation. Hence more weight should be shifted towards the external energy.

2.2 Canny Edge Detection

The Canny algorithm will first smooth the data (by means of a Gaussian filter) in order to remove speckle noise. Then edge detection is performed. Canny optimizes edge-response with respect to three criteria:

- *Detection*: real edges should not be missed, and false edges should be avoided.
- *Location*: the edge response should lie as close as possible to its true location.
- *One-response*: a true edge should not give rise to more than one response.

Canny is particularly susceptible to input parameters [6]. These parameters allow for fine-tuning of the edge-detection mechanism, permitting the user to acquire the desired results on an image data set. Canny uses a technique called "*non-maximum suppression*" that relies on two thresholding values (lower and upper). The lower defines a threshold for all points that should not be considered lying on an edge. The upper defines a threshold for all the points guaranteed to be lying on an edge [6].

To emphasize the main edges in an image, the two thresholds should be large. To find the details of an image, their value should be small. The Canny edge detector was applied with increasing lower and upper thresholds and the resulting images were probed where expected edges should exist within the US images. Canny recommends that the lower threshold should be one third the amount of the upper threshold. Our trials are consistent with the recommended values yielding a 0.2 lower threshold and a 0.6 upper threshold. We also found these thresholds reduce the creation of false edges due to speckle noise in the image without degradation.

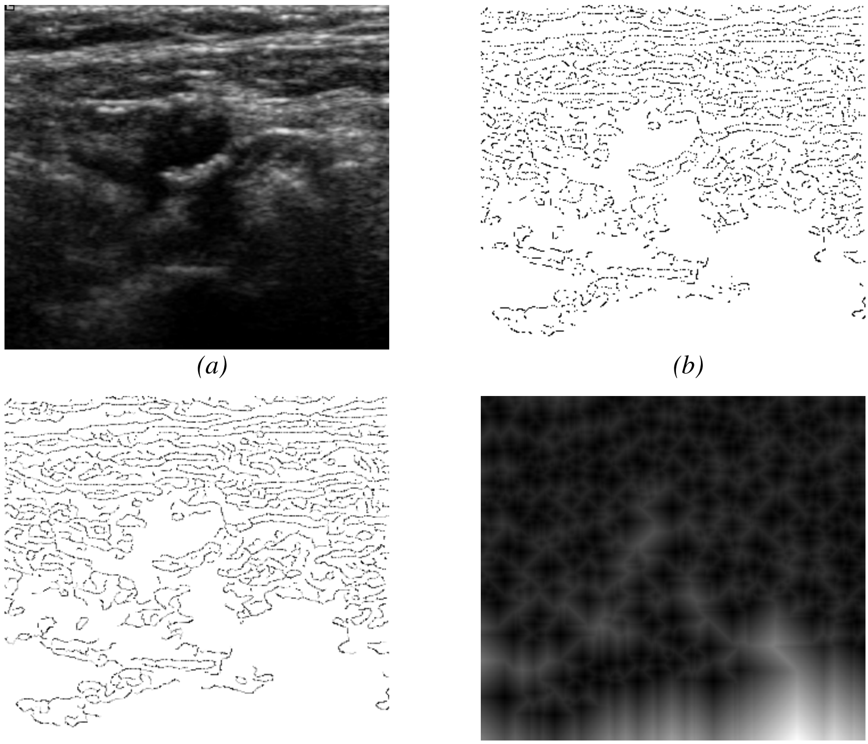

(a) (b) (c) (d)

Fig. 1. Example of Edge detection. (a) Original carotid US image. (b) Canny edge detected binary image (c) Modified Canny edge detected grayscale image (d) Distance transformed modified Canny edge detected image.

Modification to the Canny edge detection algorithm was necessary in order to more accurately integrate this measure into the external energy. The standard Canny edge detector outputs all edges as a binary result. Each point that is lying on a Canny detected edge will not have the same weight following detection; rather it will be replaced with its relative gradient. Fig. 1*(a)* shows an example of a carotid artery US image. Fig. 1*(b)* shows the US image following the application of a normal Canny edge detector. The result is a binary image with all points having the same weight. Fig. 1*(c)* shows the modified Canny edge detector where each point has a designated weight associated with its gradient – hence a gray scale image. Each gradient point is incorporated into the external energy by means of a Manhattan distance transform [17], as shown in Fig. 1*(d)*. The Manhattan distance transform provides a set of gray level intensities that show the distance to the closest boundary from each point. This provides a path to a better local minimum by avoiding small hazards of unwanted noise. The Manhattan distance of the modified Canny edge map was sufficient for the purpose of this study due to its simplicity and elegance of implementation. The energy will also converge such that it will mimic the behaviour of GVF snakes, since the curve will be forced into boundary concavities.

2.3 A-Priori Knowledge

It is desirable to incorporate some means of shape to the model without directly involving the user. Automatic shape detection takes place on the initial plots positioned by the user. This would force the active contour to converge closer to the user's first delineated points. This is especially useful in the medical arena where a specialist or technician has a clear understanding of the underlying structure being detected, such as a liver, an artery, or a heart.

Traditional shape priors in snake models tend to take place in the internal energy [12]. However, this knowledge has been incorporated into the external energy in order to influence the shape and the positional information as well – since it is readily available from the user. This shape and position information will also be represented by the Manhattan distance transform in order to properly integrate it within the external energy.

For carotid images, the prior was set to ellipses. A least squares ellipse fitting technique is performed on the points of the initial contour. The initial ellipse is defined using the initial contour placement points of the snake. Continual refinement takes place by attempting to minimize the geometric error of a series of approximating curves to the initial points. This process continues until a curve with minimal deviation from all snake contour points is found.

Fig. 2*(a)* and 2*(b)* shows the active contour being used without and with a-prior knowledge, respectively. Fig. 2*(a)* depicts an improper segment of the boundaries, most likely due to poor visualization in the lower region of the image. Fig. 2*(b)* takes the same initial plots and builds knowledge around the data by ellipse fitting in order to prevent the collapse of the curve and improve alignment with the true lumen.

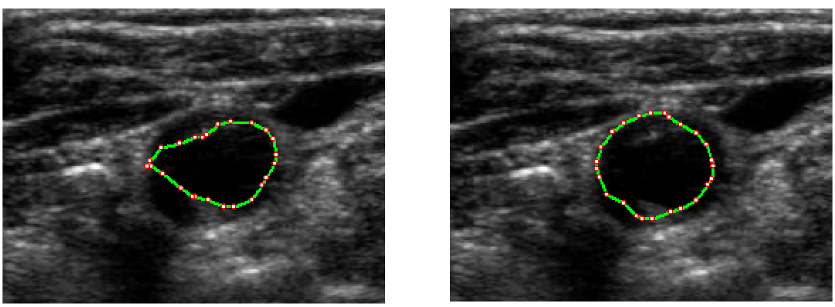

(a) *(b)*

Fig. 2. Active contour on a carotid ultrasound image. *(a)* without α-priori knowledge. *(b) with* α-priori knowledge.

2.4 Clinical Metrics

The desire to use the proposed technique in the clinical arena is paramount. One such metric is the *North American Symptomatic Carotid Endarterectomy Trial* (NASCET). This is a confirmed clinical test that may benefit patients with high-grade carotid stenosis [14]. The NASCET percent stenosis criterion is measured as: the

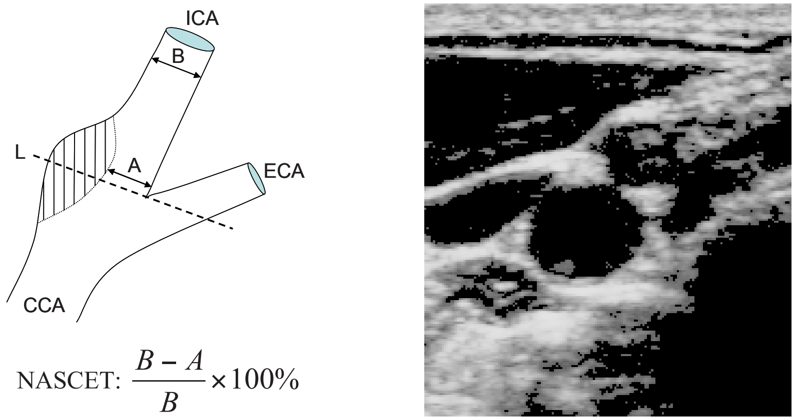

(a) *(b)*

Fig. 3. *(a)* Drawing of nascet criteria for evaluation of carotid stenosis: *A* is the diameter of the residual lumen at the point of maximal stenosis (vertical lines representing plaque); *B* is the diameter of the normal artery distal to the stenosis. (CCA, ECA and ICA stand for *Common*, *External* and *Internal Carotid Artery*, respectively) *(b)* Ultrasound image of a cross-sectional slice, at line L in *(a)*, showing the area of the carotid. Image is histogram equalized for better visualization.

diameter of lumen at the point of maximal stenosis, subtracted from the diameter of the lumen of the normal internal carotid artery, divided by the normal internal carotid artery multiplied by 100% [14]. The diameter of maximal stenosis is most often found just above the carotid bulb, near the bifurcation of the internal and external carotid arteries. A visual representation of this is shown in 4*(a)*. This test is generally performed by catheter angiography – an invasive technique requiring surgery. In this paper, we propose an alternative method of measurement from a transverse segmented US image.

While, angiography will give a 2D representation on a *longitudinal* view of any given artery, yet it will not reveal any information on the depth of that artery. Depth can be measured by taking a cross-sectional area (*transverse*) slice of the carotid, as shown in Fig 3*(b)*. This additional information should improve the traditional NASCET measurements. However, slight modification to our measurements is needed in order to conform to the NASCET standard. Since NASCET percent stenosis is based on artery diameters, where the proposed measure is based on areas, (in a generally elliptic fashion) each contour would be square rooted before the ratio is calculated. This will help to preserve the ratio of percent stenosis in a range that traditional clinicians are already familiar with, rather than introducing an entirely new range for stenosis.

3 Results

In this study, 91 carotid artery US images are used. These images include normal and diseased carotid arteries at different positions along the carotid artery, e.g., common

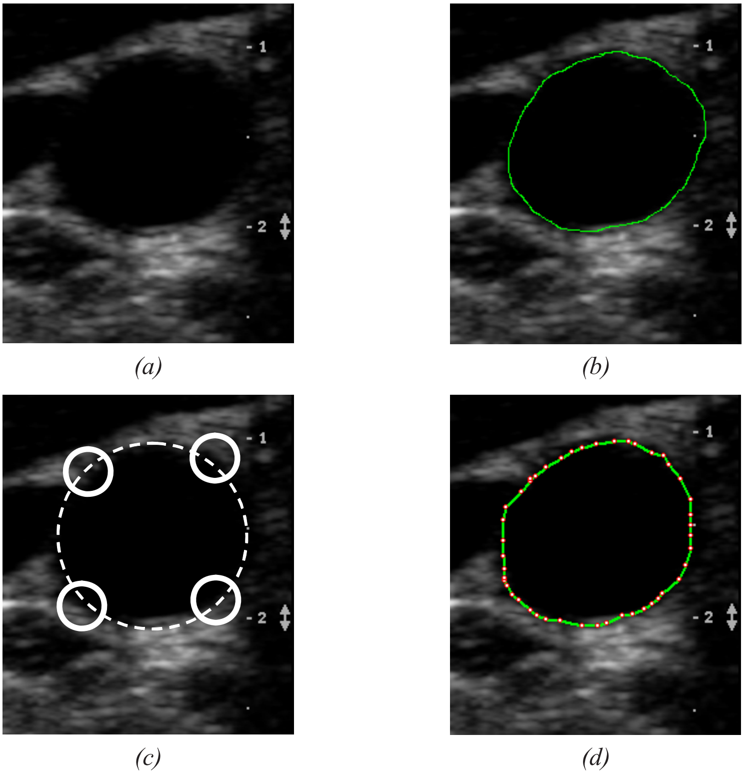

Fig. 4. Transverse carotid artery US images of the carotid bulb. *(a)* the original image. *(b)* the original image manually segmented by a clinical radiologist. *(c)* original image with four points – white circles – placed by the clinical radiologist as an initial value for the algorithm and the extracted prior ellipse as a dashed line. *(d)* the resulting segmentation by the proposed active contour algorithm.

carotid, carotid bulb, and internal carotid. Manual carotid lumen segmentation was performed on all of the images by a clinical radiologist. The images were then segmented by the proposed snake algorithm. These images were acquired using a SONOS 5500 by Philips Medical System.

Fig. 4*(a)* shows a transverse 2-dimensional US image of the carotid bulb. Fig. 4*(b)* represents the manually segmented region of the carotid bulb by a clinical radiologist at the given A position designated by the NASCET measure (as shown in Fig. 3*(a)*). Fig. 4*(c)* shows an example set of the four initial points plotted by the radiologist as an input to the active contour and the result of initial ellipse extraction. These points should be placed anywhere on the carotid lumen edge. They are required in order to achieve an elliptical approximation and the initial contour. Each point placed is automatically connected to its closest neighbour by means of a direct line of equally distanced points. Fig. 4*(d)* shows the result of the active contour following convergence. Similarly, Fig. 5*(a)*, *(b)*, *(c)* and *(d)* show the same for an internal carotid artery image (at location B designated by the NASCET measure). These results were ascertained by using the proposed active contour with parameters σ, l, u, α, β , γ, and τ, as 2.0, 0.2, 0.6, 0.09, 0.01, 0.5 and 0.4, respectively (as defined in Section 2.1).

All images processed by the proposed algorithm were examined and reviewed by a radiologist in a double blind study in order to insure the segmentations were accurate. Due to the subjectivity in estimating the borders, the radiologist reported that the proposed technique would accurately objectify the inconsistencies among clinical practitioners. This will serve to improve the computation of percent stenosis and other measures used in the clinical arena.

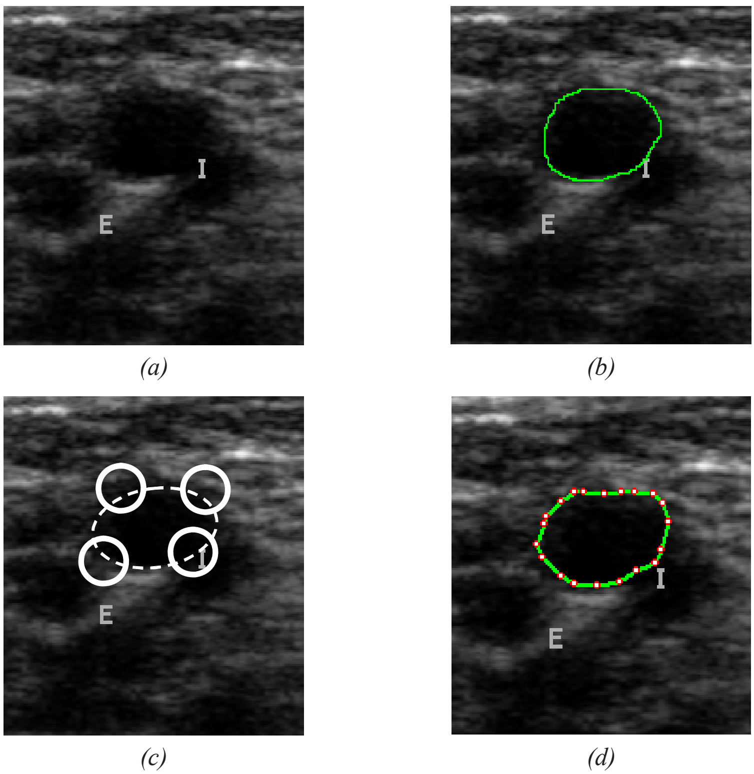

Fig. 5. Transverse carotid artery US images of the internal carotid artery. *(a)* the original image. *(b)* the original image manually segmented by a clinical radiologist. *(c)* original image with four points – white circles – placed by the clinical radiologist as an initial value for the algorithm and the extracted prior ellipse as a dashed line. *(d)* the resulting segmentation by the proposed active contour algorithm.

Overall, accuracy of the proposed system was measured by comparing the 91 cases to the expert manual segmentations by the radiologist. These measurements include both type I and type II errors as defined in [15]. Since the images at hand were mainly small segmented foregrounds against vast backgrounds, the system would best be measured by means of its *sensitivity* and *precision rate*. Sensitivity is the number of true positives divided by the number of true positives plus false negatives. In other words, it classifies how well a binary classification test correctly identifies a condition. Precision rate is the number of true positives divided by the number of true positives plus false positives. In other words, it classifies how accurate the results of the test are versus its inaccuracies. Sensitivity of the system, given a 95% confidence interval, yields 0.871 – 0.916. Whereas, precision rate, given the same confidence interval, yields 0.866 – 0.903. It is worth mentioning that these reported performance measures are quite high. This can be attributed to the fact that the initial points to the proposed system were plotted by the specialist.

4 Conclusions

In this paper, a modified DP snake algorithm helped alleviate the inherent difficulties in segmenting ultrasound carotid artery images, such as avoiding speckle noise and contour bleeding. The proposed alterations utilized a modified Canny edge detector and a-priori knowledge. Experimental results show that these alterations tune the original DP snake model in order to be used in the medical arena so that clinical analysis results can be improved.

A radiologist verified that this objective segmentation scheme would improve the calculation of different clinical measures, such as percent stenosis, by reducing the inconsistencies and variability between clinicians while reducing the time for clinician interaction. We have shown that the segmentation of the carotid artery is robust enough to be used in a clinical setting for specific domain applications.

Contributions

Author contributions are allocated as follows: research, development, implementation and paper writing were done by Ali Hamou, M.Sc., and Mahmoud El-Sakka, Ph.D. Result validation was done by Said Osman, M.D., FRCPC.

Acknowledgements

This research is partially funded by the *Natural Sciences and Engineering Research Council of Canada* (NSERC). This support is greatly appreciated.

References

[1] Abdel-Dayem, A., El-Sakka, M.: A Novel Morphological-based Carotid Artery Contour Extraction. In: Canadian Conference on Electrical and Computer Engineering, pp. 1873–1876. IEEE Computer Society Press, Los Alamitos (2004)

[2] Abdel-Dayem, A., El-Sakka, M., Fenster, A.: Watershed Segmentation for Carotid Artery Ultrasound Images. In: International Conference on Computer Systems and Applications, pp. 131–139. IEEE Computer Society Press, Los Alamitos (2005)

[3] Abdel-Dayem, A., El-Sakka, M.: Carotid Artery Ultrasound Image Segmentation Using Fuzzy Region Growing. In: Kamel, M., Campilho, A. (eds.) ICIAR 2005. LNCS, vol. 3656, pp. 869–878. Springer, Heidelberg (2005)

[4] Abolmaesumi, P., Sirouspour, M., Salcudean, S.: Real-Time Extraction of Carotid Artery Contours from Ultrasound Images. In: Computer Based Medical Systems 2000, pp. 181–186. IEEE Computer Society Press, Los Alamitos (2000)
[5] Amini, A., Tenran, S., Weymouth, T.: Using dynamic programming for minimizing the energy of active contours in the presence of hard constrains. In: 2nd International Conference of Computer Vision, pp. 95–99. IEEE Computer Society Press, Los Alamitos (1988)
[6] Bresson, X., Vandergheynst, P., Thiran, J.: A priori information in image segmentation: energy functional based on shape statistical model and image information. In: International Conference on Image Processing, vol. 3, pp. 425–428. IEEE Computer Society Press, Los Alamitos (2003)
[7] Canny, J.: Finding lines and edges in images. MIT Press, Cambridge (1983)
[8] Cohen, I.: On active contour models and balloons. Image Understanding 53, 211–218 (1991)
[9] Hamou, A., El-Sakka, M.: A Novel Segmentation Technique For Carotid Ultrasound Images. In: International Conference on Acoustics, Speech and Signal Processing, pp. 521–524. IEEE Computer Society Press, Los Alamitos (2004)
[10] Jespersen, S., Gronholdt, M., Wilhjelm, J., Wiebe, B., Hansen, L., Sillesen, H.: Correlation Between Ultrasound B-mode Images of Carotid Plaque and Histological Examination. In: Ultrasonics Symposium, pp. 1065–1068. IEEE Computer Society Press, Los Alamitos (1996)
[11] Kass, M., Witkin, A., Terzopoulos, D.: Snakes: active contour models. In: 1st International Conference on Computer Vision, pp. 259–268. IEEE Computer Society Press, Los Alamitos (1987)
[12] Leventon, M., Grimson, W., Faugeras, O.: Statistical Shape Influence in Geodesic Active Contours. In: Computer Vision and Pattern Recognition Conference, pp. 316–323. IEEE Computer Society Press, Los Alamitos (2000)
[13] Mao, F., Gill, J., Downey, D., Fenster, A.: Segmentation of Carotid Artery in Ultrasound Images. In: Engineering in Medicine and Biology Society Conference, pp. 1734–1737. IEEE Computer Society Press, Los Alamitos (2000)
[14] NASCET Team: North American Symptomatic Carotid Endarterectomy Trial (NASCET). Stroke, vol. 22, pp. 816–817 (1991)
[15] Neyman, J., Pearson, E.S: On the Use and Interpretation of Certain Test Criteria for Purposes of Statistical Inference, Part I. Joint Statistical Papers, pp. 1–66. Cambridge University Press, Cambridge (1967) (originally published in 1928)
[16] O'Donnell Jr., T., Erdoes, L., Mackey, W., McCullough, J., Shepard, A., Heggerick, P., Isner, J., Callow, A.: Correlation of B-mode Ultrasound Imaging and Arteriography with Pathologic Findings at Carotid Endarterectomy. Arch Surgery 120, 443–449 (1985)
[17] Rosenfeld, A., Pfaltz, J.: Distance Functions in Digital Pictures. Pattern Recognition 1, 33–61 (1968)
[18] Sethian, J.: Level set methods and fast marching methods: evolving interfaces in computational geometry. In: Fluid Mechanics, Computer Vision, and Materials Science, 2nd edn., Cambridge University Press, Cambridge (1999)
[19] Xu, C.: Deformable Models with Application to Human Cerebral Cortex Reconstruction from Magnetic Resonance Images. Ph.D. Dissertation, Baltimore Maryland (1999)